



HAL
open science

TRIM37 is highly expressed during mitosis in CHON-002 chondrocytes cell line and is regulated by miR-223

Benjamin Brigant, Yohann Demont, Hakim Ouled-Haddou, Valérie Metzinger-Le Meuth, Sylvie Testelin, Loïc Garçon, Laurent Metzinger, Jacques Rochette

► **To cite this version:**

Benjamin Brigant, Yohann Demont, Hakim Ouled-Haddou, Valérie Metzinger-Le Meuth, Sylvie Testelin, et al.. TRIM37 is highly expressed during mitosis in CHON-002 chondrocytes cell line and is regulated by miR-223. BONE, 2020, 137, pp.115393 -. 10.1016/j.bone.2020.115393 . hal-03491125

HAL Id: hal-03491125

<https://hal.science/hal-03491125>

Submitted on 22 Aug 2022

HAL is a multi-disciplinary open access archive for the deposit and dissemination of scientific research documents, whether they are published or not. The documents may come from teaching and research institutions in France or abroad, or from public or private research centers.

L'archive ouverte pluridisciplinaire **HAL**, est destinée au dépôt et à la diffusion de documents scientifiques de niveau recherche, publiés ou non, émanant des établissements d'enseignement et de recherche français ou étrangers, des laboratoires publics ou privés.



Distributed under a Creative Commons Attribution - NonCommercial 4.0 International License

TRIM37 is highly expressed during mitosis in CHON-002 chondrocytes cell line and is regulated by miR-223.

Benjamin Brigant^a, Yohann Demont^a, Hakim Ouled-Haddou^a, Valérie Metzinger-Le Meuth^b, Sylvie Testelin^c, Loïc Garçon^a, Laurent Metzinger^{a,§} and Jacques Rochette^{a,§,*}

^aHEMATIM EA4666, Centre Universitaire de Recherche en Santé, Université de Picardie Jules Verne, Amiens, France

^bINSERM U1148 Université Paris 13-Sorbonne Paris Cité, UFR SMBH, 93017 Bobigny, France

^cMaxillo-facial surgery department, centre hospitalo-universitaire d'Amiens, avenue Laennec, 80000 Amiens, France; EA CHIMERE, université de Picardie-Jules-Verne, avenue Laennec, 80000 Amiens, France; Facing Faces Institute, avenue Laennec, 80000 Amiens,

All from France

*Corresponding author: Pr. Jacques Rochette, HEMATIM, CURS, CHU Amiens Sud, Avenue René Laennec, Salouel, F-80054, Amiens, France. Tel: (+33) 22 82 79 12, Email: jacques.rochette@u-picardie.fr

[§]These authors contributed equally to this work.

Sources of funding.

This work was funded by European Regional Development Fund (FEDER) and Région Hauts-de-France (Grant REG 14056).

Acknowledgements.

B. Brigant is grateful to the University of Picardy Jules Verne for support (Bursary GENEPIG). The authors thank Dr. SL. Thein (NLHBI-NHI, Bethesda, MD, USA) for comments on the manuscript. We thank Didier Hérent for technical assistance.

Running title.

TRIM37 expression during the chondrocyte cell cycle.

Abstract

Multiple molecular disorders can affect mechanisms regulating proliferation and differentiation of growth plate chondrocytes. Mutations in the TRIM37 gene cause the Mulibrey nanism, a heritable growth disorder. Since chondrocytes are instrumental in long bone growth that is deficient in nanism, we hypothesized that TRIM37 defect could contribute to dysregulation of the chondrocyte cell cycle. Western blotting, confocal microscopy and imaging flow cytometry determined TRIM37 expression in CHON-002 cell lineage. We showed that TRIM37 is expressed during mitosis of chondrocytes and directly impacted their proliferation. During the chondrocyte cell cycle, TRIM37 was present in both nucleus and cytoplasm. During M phase we observed an increase of the TRIM37-Tubulin co-localization in comparison with G1, S and G2 phases. TRIM37 knock down inhibited proliferation, together with cell cycle anomalies and increased autophagy, while overexpression accordingly enhanced cell proliferation. We demonstrated that microRNA-223 directly targets TRIM37, and suggest that miR-223 regulates TRIM37 gene expression during the cell cycle. In summary, our results give clues to explain why TRIM37 deficiency in chondrocytes impacts bone growth. Modulating TRIM37 using miR-223 could be an approach to increase chondrogenesis.

Keywords: TRIM37, chondrocyte, Mulibrey nanism, miR-223, cell cycle, mitosis

Highlights of TRIM37 and chondrocytes

TRIM37 is highly expressed during mitosis in chondrocytes in nucleus and cytoplasm.

TRIM37 co-localizes with alpha-tubulin during mitosis in chondrocytes.

TRIM37 knock-down induces a decrease of proliferation independently of autophagy and apoptosis.

miR-223 directly targets TRIM37 and is involved in TRIM37 regulation during the cell cycle.

1-Introduction

Longitudinal bone growth occurs at the growth plate and is regulated by proliferation and differentiation of chondrocytes, cells that synthesize cartilage that is subsequently ossified. This process is often impaired in dwarfism. Dwarfism refers to various conditions characterized by different skeletal anomalies including short skeletal growth. (reviewed in Liu et al., 2017; Samsa et al., 2017).

Short stature with facial dysmorphism from genetic origin may result from mutations in genes involved in the defect in proliferation of chondrocytes in the growth plate (Koparir et al., 2015). These features are exemplified in the Mulibrey syndrome (OMIM #253250), a rare autosomal recessive primordial dwarfism characterized by pre- and post-natal growth restriction, craniofacial features, progressive cardiopathy, liver manifestations, metabolic syndrome, and an increased risk for tumors (Karlberg et al., 2009a). In Mulibrey patients bone x-ray findings show delayed bone age, fibrous dysplasia of long bones with narrow medullary channels and a small thoracic cage (Avela et al., 2000). Loss of function mutations in the *TRIM37* gene underly Mulibrey syndrome. The *TRIM37* gene localizes on chromosome 17q22–q23 (Karlberg et al., 2009b), and is part of the *TRIM* family. TRIM37 is characterized by a RING/BBox coiled coil domain and a MATH domain localized in the C-terminal region of the protein, that is unique to TRIM37 within the TRIM family (reviewed in Brigant et al., 2018).

TRIM37 has been found to localize in peroxisomal membranes suggesting that Mulibrey nanism is a peroxisomal biogenesis disorder (Kallijärvi et al., 2002). TRIM has been identified as an E3 ubiquitin-ligase (Kallijärvi et al., 2005). The ubiquitin system plays important roles in degradation of target proteins by the proteasome but also in protein-protein interactions. More recently TRIM37-E3 ligase activity with oncogenic function has been revealed: i) TRIM37 is over expressed in a subset of cancer cells (Dong et al., 2018; Hu and Gan, 2017; Jiang et al., 2015) and, ii) promotes their transformation by mono-ubiquitination of the histone H2A (Bhatnagar et al., 2014). In addition TRIM37 ubiquitin ligase activity is required to prevent centriole reduplication and then regulates mitosis at different stages (Balestra et al., 2013).

Furthermore knock down (KD) of TRIM37 in HepG2 cells results in defective peroxisomal matrix protein import and induces apoptosis (Wang et al., 2017). It is now well established

that TRIM37 overexpression induces cell proliferation (Jiang et al., 2016), whilst TRIM37 KD suppresses cell growth rate (Tang et al., 2018) . Taken together, these results show that TRIM37 plays an important role in genome stability and open new insights into the molecular pathology of Mulibrey nanism.

Despite the fact that dwarfism is related to growth failure and that chondrogenesis provides a template during long bone growth, TRIM37 has yet to be studied in chondrocytes.

We have analyzed TRIM37 localization and expression during the CHON-002 chondrocytes cell cycle. We have studied TRIM37 KD and over-expression (OE) and show that TRIM37 deregulation impacts CHON-002 cell proliferation and autophagy. Considering *in silico* investigations and given the documented role of miR-223 in bone remodeling (M'Baya-Moutoula et al., 2015), we studied the role of miR-223 in *TRIM37* gene expression in CHON-002 line. Altogether our results suggest molecular mechanisms that could explain the short stature with facial dysmorphism observed in the Mulibrey patients.

2-Materials and methods

2-1-Cell Culture

The CHON-002 human chondrocyte cell line is derived from the long bone cartilage of an 18-week-old female fetus. The cell line (CHON-002 ATCC ® CRL-2847™) was purchased from the American Type Culture Collection (Manassas, VA, USA). The CHON-002 cell line was cultured in Dulbecco's modified Eagle's medium (Dominique Dutscher, Inc) supplemented with 0.1 mg/ml G-418, 10% fetal bovine serum (FBS; Eurobio, Inc.), 100 U/ml penicillin (PAN Biotech, Inc.) and 100 mg/ml streptomycin (PAN Biotech, Inc.) in a humidified atmosphere of 5% CO₂ at 37°C.

2-2-Human and Rat tissues

All authors attest that the study complied with the tenets of the Declaration of Helsinki and its amendments. Human cartilage was obtained with approval from the local ethical committee of Amiens Picardie Hospital. Written informed consent was obtained from the patient. Animal studies conform to the Directive 2010/63/EU of the European Commission and all protocols were approved by our Institution's Animal Care and Use Committee (CREMEAP).

2-3-Transfection:

All transfections or transductions were performed according to the manufacturer's instructions. TRIM37 KD was realised by CHON-002 infection by using lentiviral particles (Lenti ORF particles, TRIM37 GFP tagged – Origene) expressing a specific sh-RNA sequence to KD TRIM37 expression. The corresponding sequences are as follow: TL308645VA, GCTGGACTTGTAAGAAGTGTATCTGCCAT; TL308645VB- seq: AAGGAAGCA-ACAGGCAATGTGGCGAGTGC; TL308645VC, seq: CCTGAAGAAGAAGGAATGAG-TAGCGACAGTGA; TL308645VD - seq: TTCTGAAACTGGAGAGGTTACAGCCTGTAC all clones were purchased from Origene. shRNA *scramble* was used as control (purchased from TR30021V– Origene). Infections were realised during 48h with addition of polybren (6µg/mL) in the culture media.

TRIM37 overexpression (OE) was realized by transfecting the plasmid pCMV6-XL5 (TRIM37 - NM_015294 - Human Untagged Clone (Origene). The scramble condition was obtained using the empty pCMV6-XL5 plasmid (Origene). Transfection was performed for 24 h by using lipofectamine LTX plus Reagent (Thermofisher) in DMEM without antibiotics.

miRNA regulation was studied as previously described (M'baya-Moutoula et al., 2018). The HiPerFect Transfection Reagent (Applied Biosystems) was used for miRNA knock-down and overexpression. CHON-002 cells were transfected with miR-223 mimic (Syn-hsa-miR-223-3p miScript miRNA Mimic: MSY0000280 – Qiagen), miR-223 inhibitor (Anti-hsa-miR-223-3p miScript miRNA Inhibitor: MIN0000280 – Qiagen) and Scramble (All star negative control siRNA- 1027280 – Qiagen).

2-4-Antibodies:

Primary antibodies used in the study were : mouse monoclonal antibody anti-TRIM37 (Santacruz biotechnology - sc-515044 – WB: 1/250 ; IF and IFC: 1/100) ; Rabbit polyclonal antibody anti-LC3B (Novus Biologicals – NB600 1384 – WB 1/1000) ; Rabbit monoclonal antibody anti-RNF2 (Santacruz biotechnology - sc-101109 – IF: 1/200) ; Rabbit polyclonal antibody anti-alphaTubulin (Abcam - Ab 18251 – IF 1/3000) ; Rabbit monoclonal antibody anti-alphaTubulin coupled with Phycoerythrin (Abcam - ab208752 – IFC: 1/50) ; Rabbit monoclonal antibody anti-Phospho-Histone H3 (Cell signaling - (Ser10) (D2C8) –FC: 1/100 IFC: 1/50). Secondary antibodies used in the study were: Goat anti-rabbit igG-HRP

(Santacruz biotechnology -sc-2301 – WB 1/10000); Goat anti-mouse -IgGκ BP-HRP (Santacruz biotechnology - sc-516102– WB 1/10000); Donkey anti-Rabbit IgG AF647 (Abcam - Ab 150075 – IF and IFC 1/100); Donkey anti-Mouse IgG AF488 (Abcam - Ab 150105 – IF and IFC 1/100)

2-5-Plasmid construction and luciferase reporter assay:

The binding sequence in the TRIM37 mRNA 3'-UTR region of miR-223 was predicted by TargetScan (<http://www.TargetScan.org>). The reporter gene assay was performed by using a plasmid containing the TRIM37 3'-UTR in pEZX-MT06 vector (obtained from Genecopoeia, USA). The TRIM37 3'-UTR sequence was mutated by using the QuikChange Site-Directed Mutagenesis Kit (Agilent, USA). CHON-002 cells were co-transfected with miR-223 (scramble, mimic or anti) and TRIM37 3'-UTR-pEZX-MT06 (MUT or WT) for 48 h with HiPerFect Transfection Reagent (Applied Biosystems, USA) and then harvested. Luc-Pair Duo-Luciferase HS Assay Kits (Genecopoeia, USA) was utilized to calculate the luciferase activity using Renilla luciferase signal as the internal reference of Firefly luciferase.

2-6-RNA extraction and RT-Q-PCR

RNA isolation from cell culture was performed with the miRNeasy mini Kit (Applied Biosystems), according to the manufacturer's instructions. SYBR green assays (Applied Biosystems) were used for cDNA synthesis and real-time PCR. GAPDH was used as endogenous control. Taqman assays (Applied Biosystems, USA) were used for cDNA synthesis and real-time PCR (RT 5X: U6 snRNA RT001973 – has-miR-223 RT002295; Q-PCR 20X U6 snRNA TM001973 – has-miR-223 TM000526). U6 was used as endogenous control, as previously described (M'baya-Moutoula et al., 2018). For mRNA quantification primers were obtained from Eurogentec (Belgium). Real-time PCR was performed with a Quantstudio 7 Setup (Applied Biosystems).

Table 1. Primers used in this study.

<u>gene</u>	Forward sequence	reverse sequence
<u>GAPDH</u>	AAGGTGAAGGTCGGAGTCAA	CTTGACGGTGCCATGGAATT
<u>TRIM37</u>	TCAGCTGTATTAGGCGCTGG	ACTTCTTCTGCCCAACGACA
<u>CDC25b</u>	ATTCTCATCTGAGCGTGGGC	ACTCCTTGTAGCCGCCTTTC

2-7-Immunofluorescence

To analyse the localization of TRIM37 and its co-localization with α -tubulin, cells were grown on LabTek slides. CHON-002 cells were treated for 4h with or without nocodazole, a microtubule inhibitor (1 μ g/m, 120630, Abcam). Cells were fixed and permeabilized 20 mins using the cytofix/Cytoperm plus Kit (BD Biosciences) and exposed in BSA for 30 mins. The slides were incubated with primary antibodies for 12h at 4°C in the dark. The corresponding fluorescent dye-conjugated secondary antibody was incubated for 1h at room temperature. Nucleus was stained with DAPI (Thermofisher D1306 - 1mg/mL - 1/1000) and actin was stained with Cytopainter Phalloidin-iFluor594 (Abcam - AB176757 – 1/1000).

2-8-Imaging Flow Cytometry (IFC)

CHON-002 (1 \times 10⁶) cells were fixed and permeabilized (cytofix/Cytoperm plus, BD Biosciences). Cells were re-suspended in 100 μ L of Perm/Wash Buffer (cytofix/Cytoperm plus, BD Biosciences,USA) with TRIM37 primary antibody for 1 hour. Cells were washed and incubated with specific secondary antibody, anti-tubulin-PE, DAPI and anti-P-histone-H3-APC antibody for 30 minutes at room temperature. Multispectral imaging flow cytometry was performed on an AMNIS ImageStream X Mark II equipped with 375-, 488-, and 642-nm lasers using the 40x magnification lens.

INSPIRE software v200.1.388.0 was used to record whole cells event gated on aspect ratio vs area of bright field. Cell analysis was done with IDEAS software v6.2.64.0. Only focused events were included in the analysis by using the gradient RMS feature of bright field images. Saturated signals in fluorescence channels and raw centroid X cut objects were eliminated. Cell cycle status was assessed using DAPI intensity. DAPI allows to discriminate between G1, S and G2/M phases. P-histone H3 staining was used to discriminate G2 phase to M phase. DAPI images were acquired in channel 01, Tubulin in channel 02, TRIM37 in channel 03, Brightfield in channels 04, P-Histone H3 in channel 05 and SSC in channel 06. Single color controls for each of the specific markers at the concentration used above were also acquired with Brightfield and 782 laser turned off and subsequently used for compensation.

2-9-Western Blotting

Cells were collected with RIPA Buffer (Sigma Aldrich, MS, USA). The protease inhibitor cocktail (Sigma Aldrich - P8340 – 1/100) was added. Lysates were centrifuged at 12,000g at 4 °C for 20 mins and supernatant was collected for protein quantification and western blot analysis. Equal amounts of protein (40 µg) were resolved by SDS-PAGE on 10% polyacrylamide gels. Then, the proteins were transferred to a nitrocellulose membrane (Amersham Bioscience). Membranes were further blocked for 1 h with 5% non-fat dry milk in Tris-buffer (1×) containing 0.01% Tween 20 (TBST). Membranes were then incubated with primary antibodies overnight at 4°C. Rabbit anti-GAPDH was used as control. We have revealed the TRIM37 gene product by immunoblotting with a specific monoclonal antibody (Santacruz biotechnology - sc-515044 - 1/250) raised against an internal polypeptide (amino acids 152-451) of the predicted human TRIM37 protein (964aa) (Wang et al., 2018) Horseradish peroxidase (HRP)-linked goat anti mouse antibody and goat anti rabbit antibody were used at dilution 1:5000. After washing with TBST, membranes were revealed by using an enhanced chemiluminescent reagent (SuperSignal West Pico PLUS, ThermoFisher Scientific) for 3 mins. Secondary antibodies were purchased from Santa Cruz biotechnology.

2-10-Flow cytometry:

Cell viability was measured by flow cytometry using annexin-V-phycoerythrin (PE) and 7-amino-actinomycin (7-AAD) staining kit (BD Biosciences) according to the manufacturer's recommendations. After 15 minutes of incubation, flow cytometry analysis was conducted using a MACSQuant® Analyzer 10 (Miltenyi Biotec) cytometer and apoptotic fractions were determined. Cell cycle status was assessed using DAPI and P-histone H3 stain. Briefly, 3×10^5 cells were fixed and permeabilized (Fix and perm BD Biosciences), suspended in 100µL of Buffer with 1 µl of DAPI and 1µL of P-histone H3 stain for 45 minutes at room temperature and 10 000 viable events were analyzed in the cytometer. Flow cytometry data were analyzed using the FlowJo software (Treestar). Experiments were repeated in three independent biological replicates.

2-11- Cell sorting:

CHON-002 cell cycle phase was determined by adding Nuclear-ID Red DNA stain (Enzo Life Sciences, ENZ-52406, USA). Cells were without fixation and permeabilization. A 250-fold

dilution of NUCLEAR-ID Red DNA Stain was performed to explore live cell cycle DNA. Cells were sorted according to their cell cycle phases by using a FACS Aria flow cytometer running FACSDiva software (BD Biosciences, France). After cell sorting, cells were washed with PBS 1x and mRNA was directly extracted for analysis.

2-12-Statistics:

Data are expressed as mean \pm Standard Error of the Mean (SEM). The statistical significance of differences between the experimental and control groups was evaluated by independent Student's *t* test when we compared control to TRIM37 KD or OE condition, or by the ANOVA test with Tukey's test when three or more means were compared. Statistical analysis was performed using GraphPad Prism version 6.01 for Windows (GraphPad Software, La Jolla California USA).

3-Results:

3-1-TRIM37 is expressed in CHON 002 cell line and localizes to cytoplasm and nucleus

TRIM37 protein was present in human cartilage, in mesenchymal stem cells (MSC), in the CHON-002 cell lineage and in different Rat tissues. In all cases Western blot revealed a 95 Kd protein (fig 1A) corresponding to the 964 aa product in human (Wang et al., 2017). In Rat tissues as in human MSC a supplementary reacting protein (110kd) was detected.

We studied TRIM37 expression in CHON-002 cells using confocal microscopy in order to precise its cell localization. We stained in parallel RNF2, a well-characterized E3-ubiquitin ligase used as a positive control of cytoplasmic proteins and DNA using DAPI as a nuclear marker and Phalloidin for actin labelling. The distribution of TRIM37 revealed a cytoplasmic and nuclear punctuated staining pattern in contrast with RNF2 which was localized uniquely in the cytoplasm (fig 1B). In order to confirm that TRIM37 nuclear staining was not an artefact due to protein position between nucleus and microscope objective, we generated 3D images that clearly showed that TRIM37 protein was inside the nucleus (supplementary file S1).

Previous reports showed that TRIM37 was involved in cell proliferation: TRIM37 is over expressed in a subset of cancers and its KD inhibits cell proliferation. TRIM37 may be

involved in cell cycle regulation and reported to play a role in preventing centriole reduplication events (Balestra et al., 2013) and in the centrosome assembly (Meitinger et al., 2016). We thus examined TRIM37 expression in chondrocytes during cell cycle progression using IFC (fig 1C-1D- 1E).

IFC retains the ability to assess a large number of events while dealing with image analysis that allows a high input evaluation. We could not find any differences in TRIM37 expression between G1 and S phase. However, TRIM37 expression was 2.2-fold higher in M phase compared to G1 phase ($p < 0.001$ fig 1C). Representative imaging of analysis (fig 1D) showed a particularly high TRIM37 expression during mitosis in CHON-002 cells. Given this differential expression of TRIM37 in cells during the cell cycle, and its potential relevance to chondrocyte proliferation in Mulibrey patients, we decided to examine its distribution during mitosis.

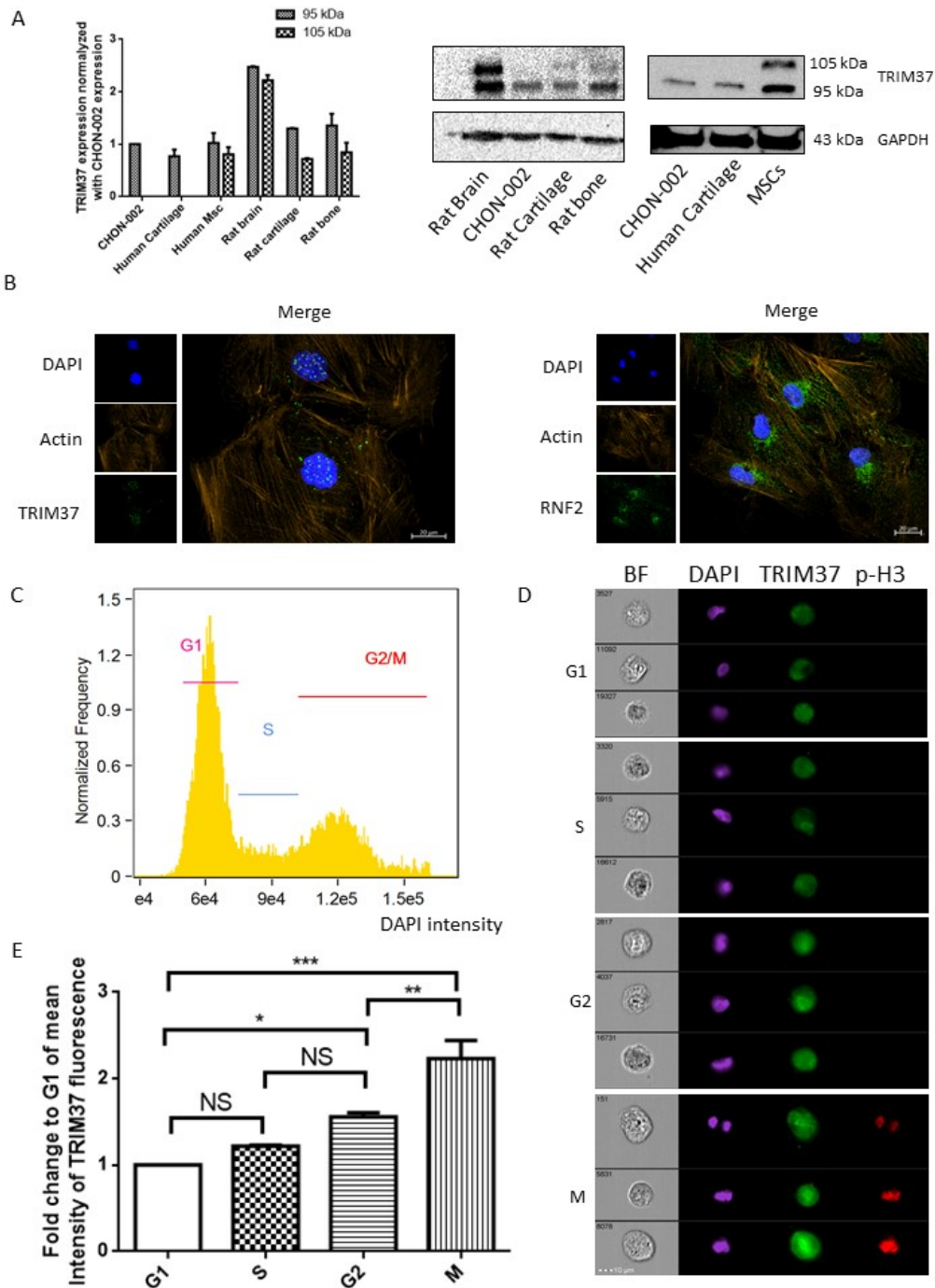


Figure 1: TRIM37 distribution and variation of expression during cell cycle. (A) Representative TRIM37 immunoblots of lysates from Rat tissues, human cartilage, MSCs and CHON-002 cell line. GAPDH was determined as the internal control. (B) Representative confocal Images. CHON-002 cells were immunostained with specific anti-TRIM37 antibody in comparison to RNF2 (cytoplasmic E3 ubiquitin ligase). Nucleus was stained with DAPI. Actin was stained with phalloidin -AF-594. Scaled bar: 20 μ m. (C) Data in the graph represent DAPI intensity and cell cycle gate (G1, S and G2/M) used for the DATA analysis. (D) Representative Images flow cytometry of TRIM37 during cell cycle. Blue signals represented DAPI-stained nuclei, TRIM37 (green). P-histone H3 (red), was used as an indicator of mitosis. Fluorescent cells were detected and analyzed by AMNIS ImageStream X Mark II equipped with 375-, 488-, and 642-nm lasers using the 40x magnification lens. Brightfield images were acquired in channels 04 (column 1), DAPI in channel 01 (column 2) TRIM37 in channel 03 (column 3), P-Histone H3 in channel 05 (column 4). (E) Data in the graph represent the ratio to G1 of mean of fluorescence of TRIM37 intensity in cell cycle phase. The data are expressed as mean \pm SEM from three

independent experiments. Non-Significant (NS): $P > 0.05$; * < 0.05 ; ** < 0.01 ; *** < 0.001 (Anova test with Tukey test).

3-2-TRIM37 colocalizes with alpha-tubulin during mitosis

Based on the fact that TRIM37 expression increases from G1 to M phase we also examined TRIM37 distribution during mitosis. We then examined the precise TRIM37 localization during the M-phase using IFC and IF in CHON-002 cells. As shown in fig 2A, TRIM37 assumes the form of spindles (fig 2A). Using confocal microscopy, we observed that TRIM37 colocalizes with alpha-tubulin during M phase. No colocalization was observed in the other phases or after Nocodazole treatment (fig 2B).

In order to confirm the colocalization of TRIM37 and alpha-tubulin during mitosis we also evaluated TRIM37 localization in CHON-002 cells by using IFC (fig 2C). To quantify the colocalization between TRIM37 and alpha-tubulin we used the Bright Details Similarity (BDS). This tool provided by IDEAS software is specifically designed to compare the bright details of two images and to quantify the co-localization of two probes (Pugsley, 2017). During M phase we observed an increase of the TRIM37-Tubulin colocalization in comparison with G1, S and G2 phases with respectively, $p=0.032$, $p=0.0024$ and $p=0.0061$ (fig 2D). This result confirmed that TRIM37 and alpha-tubulin increase specifically during mitosis.

The next feature to investigate with IFC is Bright Detail Colocalization 3 (BDC3) (Pugsley, 2017). BDC3 is a measurement of the co-localization of three markers/probes. The increase of BDC3 between TRIM37, alpha-tubulin and DAPI specifically during mitosis ($p < 0.001$) indicates that these three molecules share a common area during this phase (fig 2E). We next decided to modulate the expression of TRIM37 in our cell line to further expand our investigations.

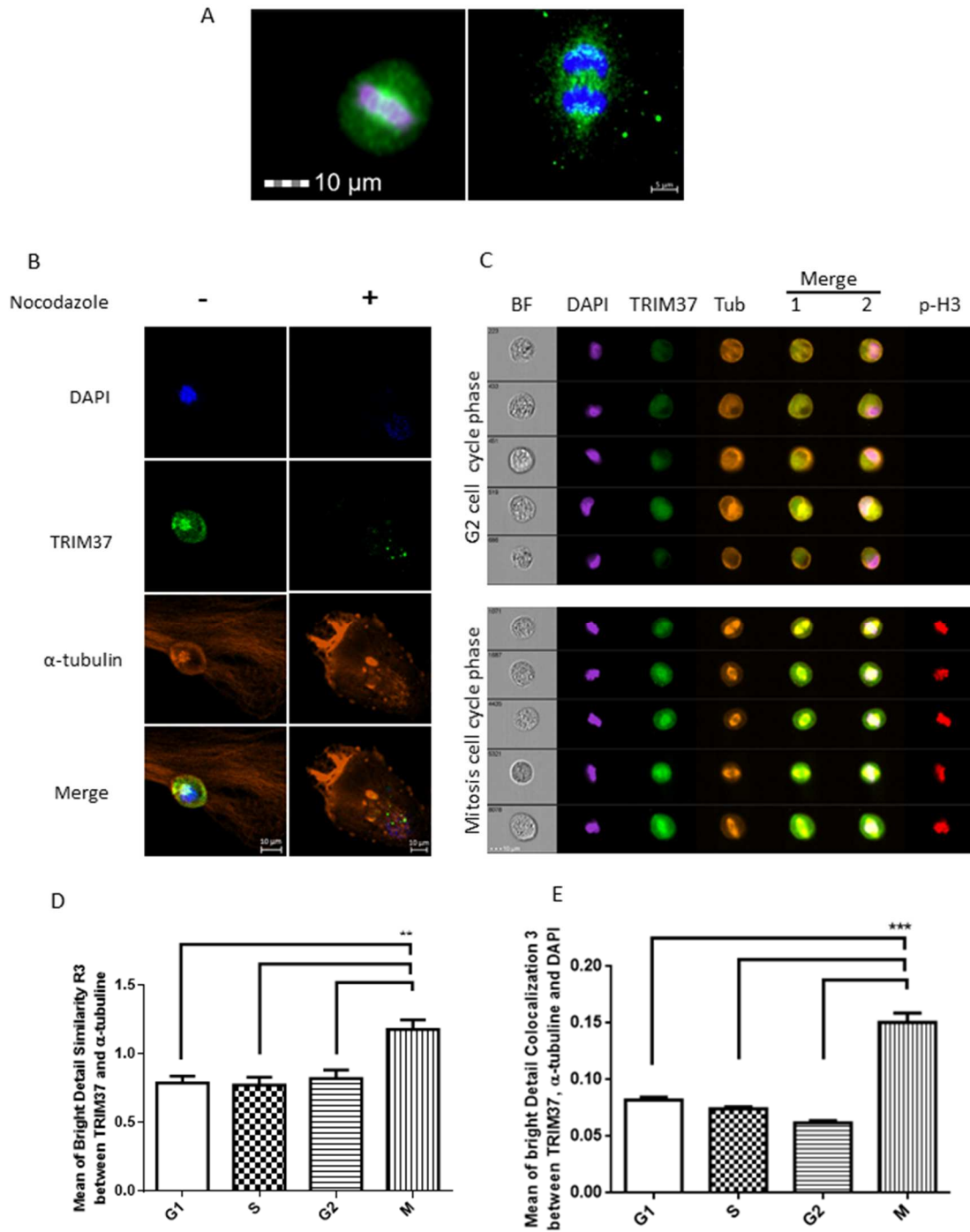


Figure 2: TRIM37 colocalizes with alpha-tubulin in CHON-002 cells. (A) TRIM37 (green) organization during mitosis, by using IFC analysis (right) and confocal microscopy (left). (B) Confocal microscopy. CHON-002 cells were treated for 4h with or without nocodazole (+/-). Cells were stained with anti-TRIM37 antibody (green) and anti-alpha-tubulin antibody (orange) and DAPI (blue). (C) Representative images of cells acquired by IFC in G2 phase and in mitosis phase. CHON-002 cells were stained with DAPI (blue), TRIM37 (green), alpha-tubulin (orange) and P-histone H3 (Red). Brightfield images were acquired in channels 04 (column 1), DAPI in channel 01 (column 2) TRIM37 in channel 03 (column 3), alpha-tubulin (column 4), merge of TRIM37 and alpha-tubulin image (column 5) merge of TRIM37 and alpha-tubulin and DAPI image (column 6) and P-Histone H3 APC in channel 05 (column 7). Scaled bar: 10μm (D) Histogram represents TRIM37 colocalization along the cell cycle. Mean of Bright detail similarity (BDS) signal between TRIM37 and α-tubulin in each cycle phase. (E) Histogram represent mean of Bright Detail Colocalization 3 between TRIM37, α-tubulin and DAPI in each cycle phase. The data are expressed as mean ± SEM from four independent experiments. ** P < 0.01 ; *** < 0.001 (Anova test with Tukey test).

3-3- Apoptosis and autophagy depend on TRIM37 OE but are not affected by TRIM37 KD

A small hairpin RNA (shRNA) lentiviral strategy was used to specifically KD TRIM37 expression in chondrocyte cell line, while TRIM37 OE was performed by using transient expression. Western blot analysis showed a 60% decrease in TRIM37 protein expression level in KD condition (fig 3A) and a 50% increase in TRIM37 protein expression level in overexpression condition (fig 3B).

We tested if TRIM37 KD or OE could affect CHON-002 cell viability. By using DAPI staining, we found that neither OE nor KD affect cell mortality in our experimental conditions (fig 3C). Since it has been recently shown that TRIM37 deficiency enhances apoptosis (Wang et al., 2018), we quantified apoptosis in CHON-002 cell culture in OE and KD conditions by using cytometry with annexin 5 immunostaining. We found that OE overexpression significantly decreases the percentage of cells going into apoptosis while TRIM37 KD does not modify this percentage when compared to the control (fig3C).

Because there is a crosstalk between the ubiquitin system and autophagy (Ji and Kwon, 2017) with TRIM37 depletion increasing basal autophagic flux (Wang et al., 2018) we studied LC3-II expression, a marker of autophagy, in CHON-002 cells

In TRIM37 depleted cells in presence of amiodarone we found an increase in LC3-II expression when compared to control. On the other hand, amiodarone treatment did not induce any LC3-II change when compared to results obtained without amiodarone. This result suggests that TRIM37 KD could promote autophagy (fig 3D). In TRIM37 OE conditions (lipofectamine transfection) autophagy was induced by lipofectamine transfection. As expected, it should be noticed that in TRIM37 OE conditions LC3-II was decreased in comparison with control cells (fig 3E). To summarize, we show that TRIM37 OE prevents autophagy.

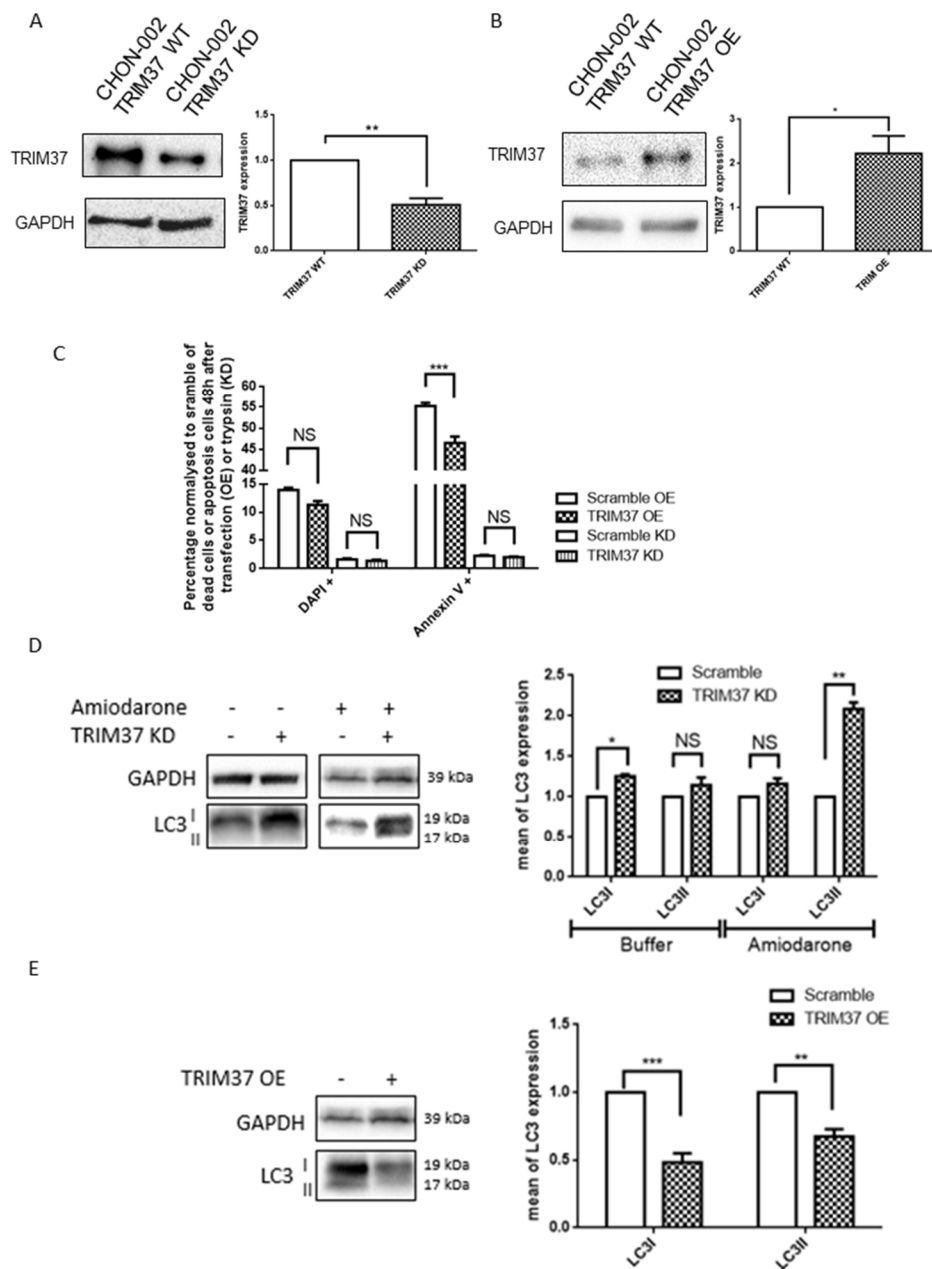


Figure 3: TRIM37 modulation and variation of cell death. (A) Effects of transduction of specific shRNAs on TRIM37 expression in CHON-002 cells. Cells were infected with lentiviral particles containing control shRNA sequence (Scramble) or specific sequence complementary to TRIM37 (TRIM37 knock down (KD)); TRIM37 expression was measured by Western blot analysis. GAPDH was determined as the internal control. One representative blot is shown out of three independent experiments (Student's t-test). (B) Effects of transfection of specific TRIM37 vector in CHON-002 cells. Cells were transfected with lipofectamine containing control sequence (Scramble) or specific sequence of TRIM37 (TRIM37 overexpression (OE)); TRIM37 expression was measured by Western blot analysis. GAPDH was determined as the internal control. One representative blot is shown out of three independent experiments (Student's t-test). (C) Histogram showing effect of TRIM37 KD or OE on cell mortality (DAPI +) or apoptosis (Annexin5 +). Cells were cultured in DMEM. After 48 hours cell mortality was assayed with DAPI staining and apoptosis with annexin5 by flow cytometry (FC) (Student's t-test). (D) Effect of TRIM37 KD on autophagy estimated with LC3I and LC3II quantification with or without autophagy activator (Amiodarone). (E) Effect of TRIM37 OE on autophagy estimated with LC3I and LC3II quantification (Student's t-test). The data are expressed as mean \pm SEM from three independent experiments. Non-Significant (NS): $P > 0.05$; * < 0.05 ; ** < 0.01 ; *** < 0.001 .

3-4-TRIM37 modulates proliferation of CHON-002 cells.

Based on the fact that TRIM37 expression is up regulated in many cancer cells we next studied the consequence of TRIM37 depletion and OE on chondrocyte cell proliferation. We found that TRIM37 depletion reduces cell proliferation (fig.4A). In TRIM37 KD condition MTT tests were realised with 3MA (autophagy inhibitor), and levels were significant decreased from day 2 with or without autophagy inhibitor. Conversely to KD results TRIM37 OE increased proliferation from day 3 after transient transfection (fig 4B).

The decrease in cell proliferation in TRIM37-depleted cells was related to a decreased number of mitotic cells division when compared to wild type cells, as measured using PH3A staining on FC (fig 4C). In TRIM37-depleted cells we observed a significant increase in the percentage of cells in S phase. This suggests that TRIM depletion could induce a blockage leading in S phase to a decrease of mitotic cells. Over expression of TRIM37 increased the mitotic rate and reduced the percentage of cells in S phase (fig 4D).

In the next step of our experiments, we tried to identify regulators of the expression of TRIM37.

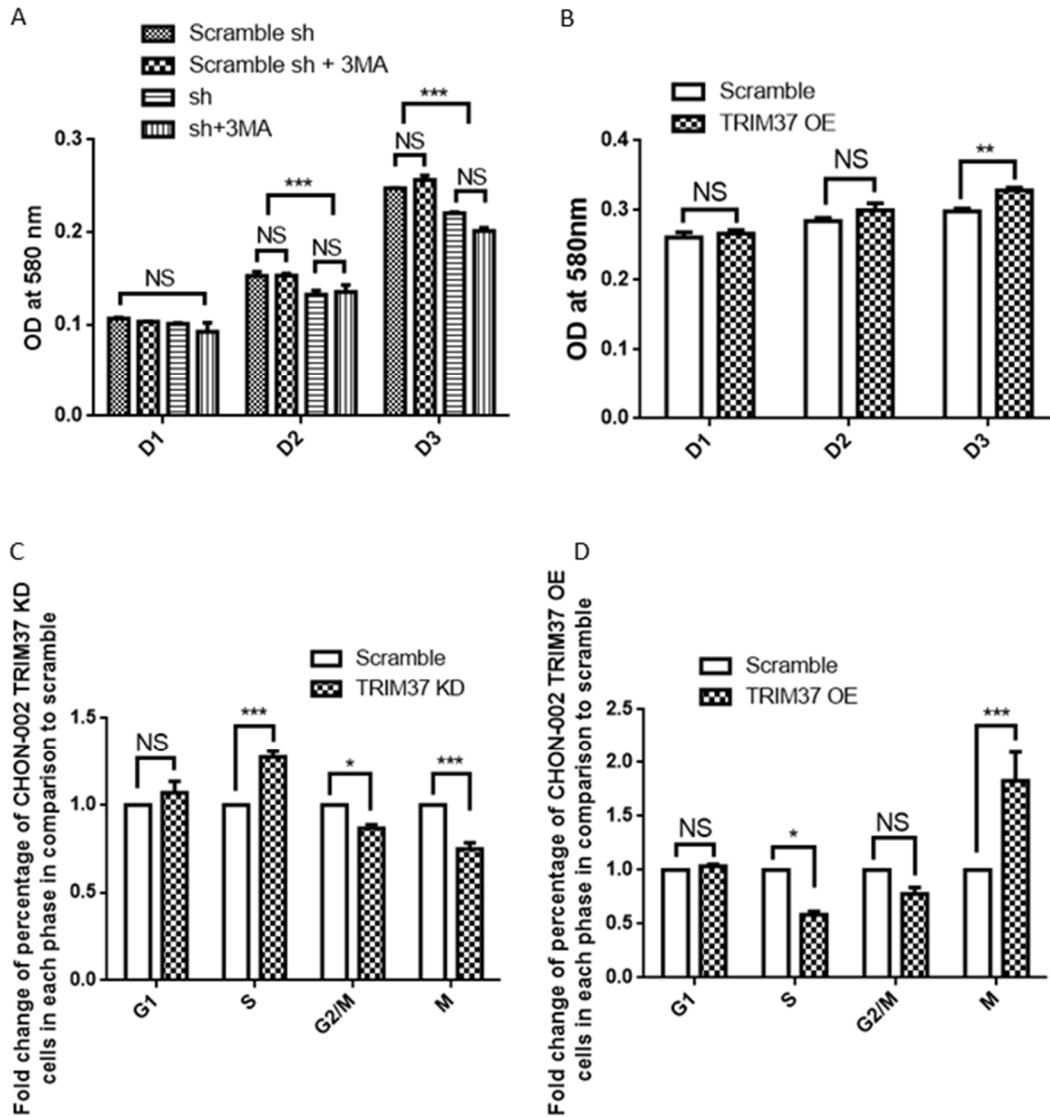


Figure 4: TRIM37 modulates proliferation in CHON-002. (A and B) Estimation of proliferation with MTT method is presented as the mean of optical density (OD) (2way Anova). Cell proliferation with or without autophagy inhibitor 3-Methyladenine (3MA). (C and D) Histogram representing fold change of percentage of cell cycle stage in CHON-002 WT, KD and OE measured by flow cytometry. Cells were stained with P-histone-H3-APC (marker of mitosis) and DAPI (Student's t-test). The data are expressed as mean \pm SEM from three independent experiments. Non-Significant (NS): $P > 0.05$; * < 0.05 ; ** < 0.01 ; *** < 0.001 .

3-5-The microRNA-223 regulates TRIM37 in CHON-002 cells.

miR-223 has been described as important in osteoclastogenesis (M'Baya-Moutoula et al., 2015). In *silico* analyses using Targetscan version 7.2 (Agarwal et al., 2015) suggested with a context score of 98% that TRIM37 3'UTR sequence is complementary to miR-223 in its seed region. We then decided to investigate a role for miR-223 in the regulation of TRIM37 expression.

We first looked at the effect of miR-223 OE (using a pre-miR-223 RNA sequence, mimic miR-223) and KD (using an antisense RNA complementary to miR-223, anti-miR-223) in CHON-002 cells. Using RT-Q-PCR, we determined miR-223 levels, to check the efficiency of the transfections. We found that miR-223 mimic increased miR-223 expression more than 700-fold while anti-miR-223 decreased miR-223 expression of about 60% (fig 5A).

By using western blotting analysis, we showed that miR-223 OE (by mimic miR-223) induced a decrease of approximately 30% in TRIM37 expression, whereas anti miR-223 increased significantly TRIM37 expression by approximately 40% (fig 5B). Our results suggest thus that miR-223 regulates TRIM37 expression.

Luciferase reporter assays were conducted to verify that TRIM37 binds to miR-223-3p directly. TRIM37-3'UTR-WT or TRIM37-3'UTR-MUT were co-transfected with miR-223 mimics, anti-miR-223 and negative control, in CHON-002 cells. We mapped out this interaction (fig 5C). miR-223 KD induced a significant 60% increase of luciferase activity of TRIM37-3'UTR-WT whereas mimic miR-223 decreased it by approximately 40% (fig 5D), indicating that miR-223 binds TRIM37-3'UTR and regulates directly its target gene TRIM37. Mutating the 3'UTR sequence abolished totally this effect (Figure 5D). Altogether, our data show that miR-223 binds in a complementary way the specific TRIM37 mRNA 3'-UTR binding site to regulate its expression.

Since a negative feedback loop has previously been described with miR-223 and the transcription factor NFIA (Taïbi et al., 2014), we evaluated whether TRIM37 could regulate miR-223 intracellular levels. TRIM37 overexpression in our cellular model decreased miR-223 intracellular levels while TRIM37 knock-down induced a strong enhancement in miR-223 levels (fig 5E).

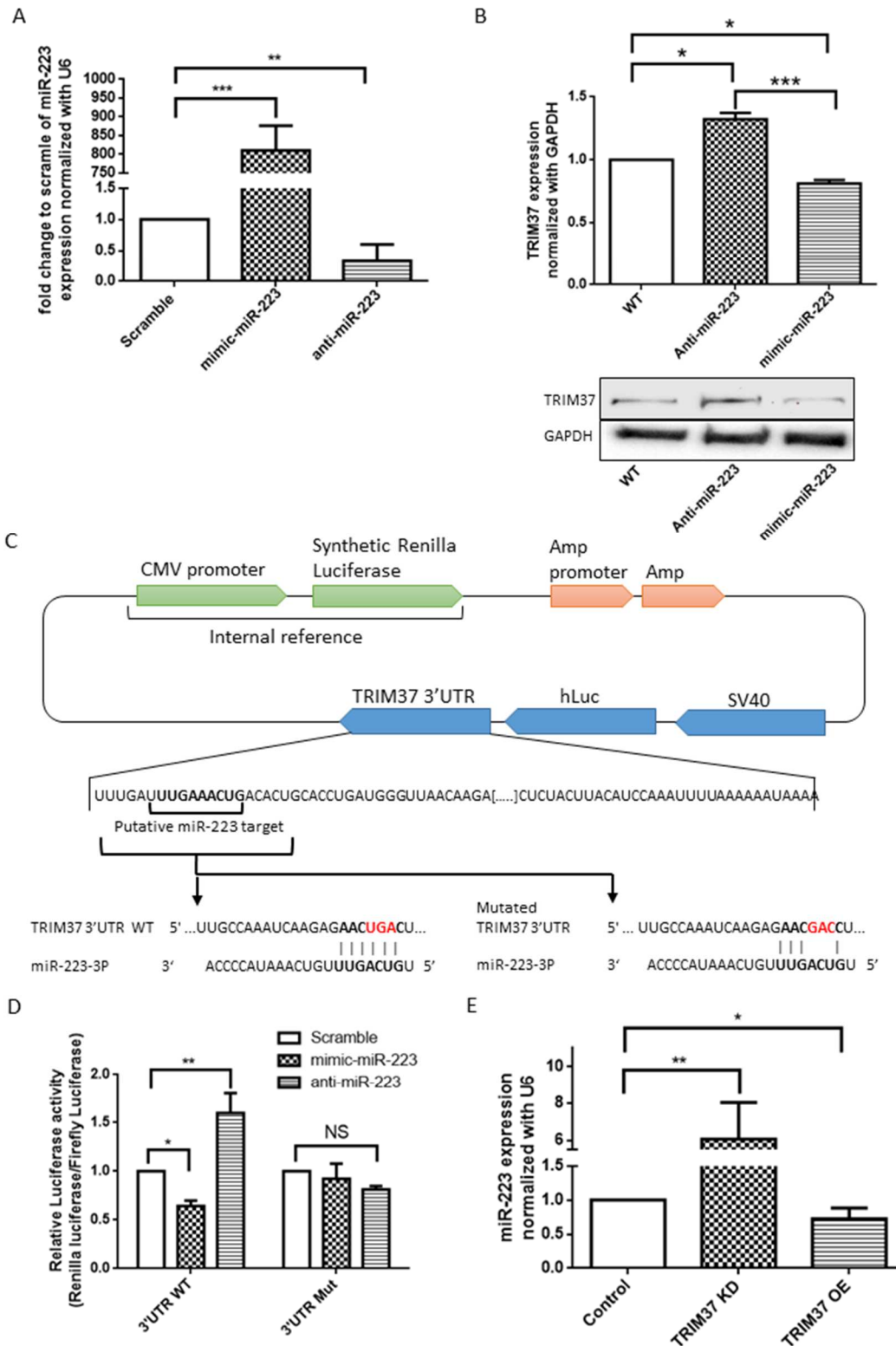


Figure 5: miR-223 regulates TRIM37 protein expression. (A) miR-223 expression determined by RT-qPCR after transfection of miR-223 mimic, anti or scramble. Results were normalized with U6 (Student's t-test). (B) TRIM37 expression after miR-223 modulation by western blot. GAPDH was determined as the internal control (Student's t-test). (C) Predicted target region for miR-223 in TRIM37 3'UTR (in bold). Mutagenesis site is highlighted in red. (D) Luciferase gene reporter assay with 3'UTR TRIM37 WT or mutated (2way Anova). (E) miR-223 expression in CHON-002 WT, TRIM37 KD and OE (Anova test with Tukey test). The data are expressed as mean \pm SEM from three independent experiments. Non-Significant (NS): $P > 0.05$; * < 0.05 ; ** < 0.01 ; *** < 0.001 .

We next looked at the expression of miR-223 and TRIM37 during the chondrocyte cell cycle, taking into account its importance in Mulibrey patients' chondrogenesis.

3-6-miR-223 participates in cell cycle regulation by TRIM37.

We next studied more precisely the link between miR-223 expression and TRIM37 levels during the successive phases of the cycle of the CHON-002 chondrogenic cells. Cells were first stained in live condition by a nuclear dye without permeabilization to preserve the RNA cellular content and then sorted according to their cell cycle stage as described in Material and Methods (fig 6A). Total RNA was extracted, reverse transcribed, and the levels of mRNA specific for TRIM37 were measured by RT-qPCR. CDC25b level, reported to increase during the cell cycle (Lindqvist et al., 2004), was quantified in parallel as a positive control. Indeed, we detected an increase in CDC25b levels, along the different phases of the cell cycle (fig 6B). TRIM37 mRNA remained stable during all the cell cycle phases, considering that nuclear staining was controlled by fluorescent microscopy in different phases (fig 6C). In contrast, TRIM37 protein expression almost doubled in G2/M phase compared to G1 and S phases, while miR-223 expression decreased during S and G2/M phases compared to G1 phases (fig 6D). This is consistent with the hypothesis that miR-223 directly regulates TRIM37 and participates to TRIM37 regulation during the cell cycle.

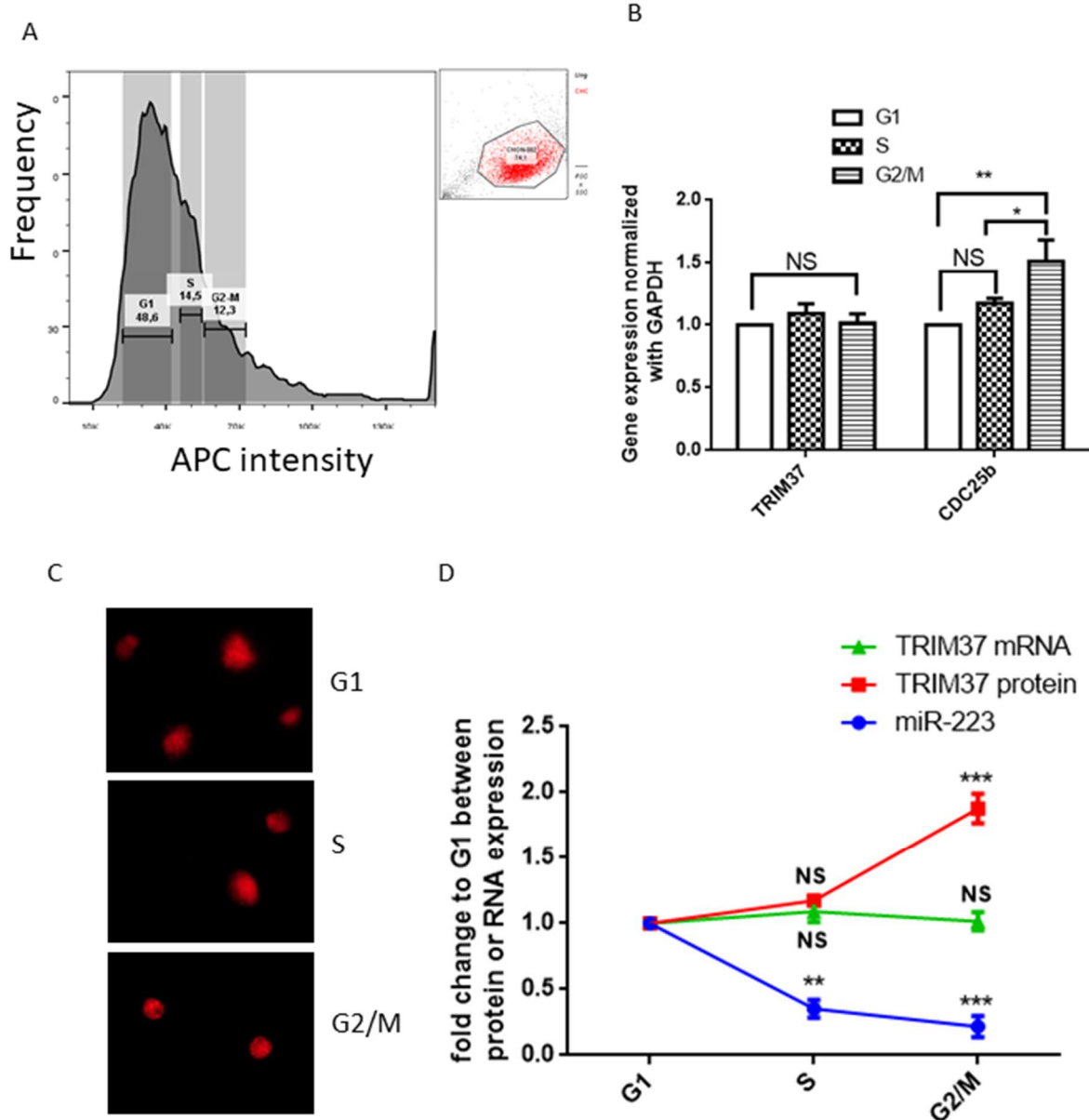


Figure 6: miR-223 regulates TRIM37 during cell cycle. (A) Cells were stained by NUCLEAR-ID Red (Enzo) in CHON-002 living cells. Cells were sorted with Fax Aria 2 cell sorter in different fractions, G1 phase, S phase or G2/M phases. (B) TRIM37 and CDC25b gene expression were determined by RT-qPCR for each cell cycle phase. (C) Representative microscopy image of nucleus stained with NUCLEAR-ID Red (Enzo), in G1 – S and G2/M. (D) Comparison of TRIM37 protein expression (IFC), TRIM37 mRNA (RT-qPCR) and miR-223 (RT-qPCR) expression in cell cycle phase. Each expression was normalised using G1 expression. The data are expressed as mean \pm SEM from three independent experiments. Non-Significant (NS): $P > 0.05$; * < 0.05 ; ** < 0.01 ; *** < 0.001 (Anova test with Tukey test).

Supplementary data:

Supplementary file S1: 3D reconstruction of confocal imaging of CHON-002 with TRIM37 stained in green, Actin in orange and DAPI in blue.

4-Discussion

This work represents to our knowledge the first study of TRIM37 function in chondrocytes. We demonstrate here that TRIM37 is expressed in CHON-002 cell line, human cartilage, Mesenchymal Stem cells (MSc) as well as in different rat tissues.

Using a monoclonal antibody we found an expression pattern in CHON-002 cell line and in human cartilage that was similar to previous results obtained with the same antibody in other cells (Wang et al., 2018). Two isoforms have been described in human and mouse: *Trim37a* (24-exon transcript) and an alternative form with an additional 3' exon (*Trim37b*). However, while the two human transcripts encode for identical protein products of 964 amino acids in mature cells, mouse *Trim37b* produces a protein product with 47 extra C-terminal amino acids, and we propose that this 1008 amino acids isoform could be also present in rat tissues. To explain the supplementary TRIM37 protein band revealed in human MSCs we hypothesize the presence of a post translational modification compatible with TRIM37 auto-monoubiquitination (Kallijärvi et al., 2005).

We found that TRIM37 is expressed in the nucleus of CHON-002 cell line, in addition to its previously published localization in the cytoplasm (Kallijärvi et al., 2002). In the present work, we showed that TRIM37 is expressed during mitosis of a chondrocyte cell line and directly impacts their proliferation. We determined that TRIM37 is over-expressed during the mitosis phase, compared to the other phases of the cell cycle using IFC. During interphase, cells display one centrosome, then the centrosome is duplicated during the S phase and becomes the pole of the spindle at mitosis (Nigg and Holland, 2018). Regulation of centriole number with prevention of the centriole replication events has been assigned to TRIM37 (Balestra et al., 2013), as the loss of TRIM37 makes spindle assembly more robust to centrosome removal (Meitinger et al., 2016). The co-localization of TRIM37 with tubulin at the mitotic spindle together with its E3 ligase activity reinforces the important role of TRIM37 in the control of centriole homeostasis. We are aware that using an immortalized chondrocyte cell line to study cell proliferation may not utterly reflect physiological conditions *in vivo*. Our present results will have to be expanded in a future work using

primary human cells to confirm the main results and to study the impact of TRIM37 on chondrocyte differentiation. Mulibrey nanism is not the only example of primordial dwarfism that involves a centriole biogenesis or assembly control together with an E3 ubiquitin ligase property. Like TRIM37, TRAF Interacting Protein (TRAIP) exhibits an E3 ubiquitin ligase activity and is functionally required for the spindle assembly checkpoint. Homozygous mutation in the TRAIP gene is responsible for the Seckel-type 9 dwarfism (OMIM #616777) (Harley et al., 2016). Mutations in another centriole biogenesis gene *PLK4* have been described also in a subtype of Seckel syndrome (OMIM #616171). Mutations in the 3M/Cul7 E3 Ubiquitin Ligase Complex dysregulate microtubule assembly and lead to the 3M syndrome (OMIM #273750) (Yan et al., 2014). The SOFT syndrome (OMIM #614813) is due to POC1A mutation and the MPODII (OMIM #602782) syndrome is caused by mutation in the pericentrin (PCNT) gene. They are respectively related with centriole assembly and microtubule stabilization defects (Koparir et al., 2015; Luo and Pelletier, 2014).

We found that TRIM37 KD reduces mitosis and induces a repression in CHON-002 proliferation. Conversely TRIM37 OE promotes proliferation. This is in accordance with previous results indicating that TRIM37 behaves as an oncoprotein in breast cancer cells (Bhatnagar et al., 2014). We also found that TRIM37 KD promotes LC3II expression and thus autophagy in chondrocytes. This result is in accordance with the recent observation that TRIM37 depletion increases basal autophagic flux through the MTORC1 pathway (Wang et al., 2018). Autophagy is essential for the chondrocyte development and viability during endochondral ossification (Bohensky et al., 2007; Settembre et al., 2009) and genetic studies have identified potential links between human stature and autophagy (Pan et al., 2010).

miRNAs are evolutionarily conserved, 20-25 nucleotide-long non-coding RNAs, that regulate gene expression by base pairing with specific target mRNAs in the 3'UTR, in turn inducing translational repression and decreasing translation of target proteins. We previously demonstrated that miR-223 plays a role in bone remodeling (M'Baya-Moutoula et al., 2015). Furthermore miR-223 is expressed in chondrocytes (Cousty et al., 2018; Kim et al., 2014) and because miR-223 displays a complementary sequence with the seed sequence of the TRIM37 3'-UTR we have studied TRIM37 regulation expression by miR-223 in CHON-002 cell and showed that miR-223 directly regulates TRIM37 and participates to TRIM37 regulation during the cell cycle. In our overexpression condition (mimic miR-223), we obtained a decrease of approximately one third of TRIM37 expression, as evidenced by western blotting and luciferase assay. This implicates that other factors are probably involved in the regulation of TRIM37. It is well known that the UTR of mammalian mRNAs are often

targeted by more than one miRNA but also by several UTR-binding regulatory proteins (see for example review by (Bartel, 2009) MicroRNAs: target recognition and regulatory functions. In the future it would be interesting to identify other regulatory factors of TRIM37, to have a better understanding of its expression.

How TRIM37 regulates osteoblast differentiation and function remains a challenging problem. Despite the fact that the high level of expression of TRIM37 we evidenced in this study has not been documented in literature yet, it has been shown that other E3 ligases are involved in osteogenesis. Smurf1, another E3 ligase inhibits mesenchymal stem cell proliferation and osteoblastogenesis (Zhao et al., 2010) when knockdown of Wwp2 leads to significant deficiencies of osteogenesis (Shu et al., 2013). Furthermore, like TRIM37, Wwp2 has been shown to be essential for normal cell cycle progression (Choi et al., 2015). We may suspect that TRIM37 as others E3 ligases may also regulate osteoblast function at different stages of differentiation and proliferation. This could be the purpose for future investigation.

We also suggest that long term dysfunction of the chondrogenic cell cycle, due to TRIM37 defect in the Mulibrey syndrome may lead to a depletion of chondrogenic cells in these patients, in turn shortening the growth of long bones, in turn leading to nanism. Assessment of the composition of the growth plate by qualitative and quantitative flow cytometry and the availability of cells to study gene and protein expression will be of importance in further unraveling cartilage development, endochondral bone growth, and the molecular basis of inherited dwarfism.

Disclosures : None

Bibliography :

Agarwal, V., Bell, G.W., Nam, J.-W., and Bartel, D.P. (2015). Predicting effective microRNA target sites in mammalian mRNAs. *ELife* 4.

Avela, K., Lipsanen-Nyman, M., Idänheimo, N., Seemanová, E., Rosengren, S., Mäkelä, T.P., Perheentupa, J., Chapelle, A.D., and Lehesjoki, A.E. (2000). Gene encoding a new RING-B-box-Coiled-coil protein is mutated in mulibrey nanism. *Nat. Genet.* 25, 298–301.

- Balestra, F.R., Strnad, P., Flückiger, I., and Gönczy, P. (2013). Discovering regulators of centriole biogenesis through siRNA-based functional genomics in human cells. *Dev. Cell* 25, 555–571.
- Bartel, D.P. (2009). MicroRNA Target Recognition and Regulatory Functions. *Cell* 136, 215–233.
- Bhatnagar, S., Gazin, C., Chamberlain, L., Ou, J., Zhu, X., Tushir, J.S., Virbasius, C.-M., Lin, L., Zhu, L.J., Wajapeyee, N., et al. (2014). TRIM37 is a new histone H2A ubiquitin ligase and breast cancer oncoprotein. *Nature* 516, 116–120.
- Bohensky, J., Shapiro, I.M., Leshinsky, S., Watanabe, H., and Srinivas, V. (2007). PIM-2 is an independent regulator of chondrocyte survival and autophagy in the epiphyseal growth plate. *J. Cell. Physiol.* 213, 246–251.
- Brigant, B., Metzinger-Le Meuth, V., Rochette, J., and Metzinger, L. (2018). TRIMming down to TRIM37: Relevance to Inflammation, Cardiovascular Disorders, and Cancer in MULIBREY Nanism. *Int. J. Mol. Sci.* 20.
- Choi, B.H., Che, X., Chen, C., Lu, L., and Dai, W. (2015). WWP2 is required for normal cell cycle progression. *Genes Cancer* 6, 371–377.
- Coustry, F., Posey, K.L., Maerz, T., Baker, K., Abraham, A.M., Ambrose, C.G., Nobakhti, S., Shefelbine, S.J., Bi, X., Newton, M., et al. (2018). Mutant cartilage oligomeric matrix protein (COMP) compromises bone integrity, joint function and the balance between adipogenesis and osteogenesis. *Matrix Biol. J. Int. Soc. Matrix Biol.* 67, 75–89.
- Dong, S., Pang, X., Sun, H., Yuan, C., Mu, C., and Zheng, S. (2018). TRIM37 targets AKT in the growth of lung cancer cells. *OncoTargets Ther.* 11, 7935–7945.
- Harley, M.E., Murina, O., Leitch, A., Higgs, M.R., Bicknell, L.S., Yigit, G., Blackford, A.N., Zlatanou, A., Mackenzie, K.J., Reddy, K., et al. (2016). TRAIP promotes DNA damage response during genome replication and is mutated in primordial dwarfism. *Nat. Genet.* 48, 36–43.
- Hu, C.-E., and Gan, J. (2017). TRIM37 promotes epithelial-mesenchymal transition in colorectal cancer. *Mol. Med. Rep.* 15, 1057–1062.
- Ji, C.H., and Kwon, Y.T. (2017). Crosstalk and Interplay between the Ubiquitin-Proteasome System and Autophagy. *Mol. Cells* 40, 441–449.
- Jiang, J., Yu, C., Chen, M., Tian, S., and Sun, C. (2015). Over-expression of TRIM37 promotes cell migration and metastasis in hepatocellular carcinoma by activating Wnt/ β -catenin signaling. *Biochem. Biophys. Res. Commun.* 464, 1120–1127.
- Jiang, J., Tian, S., Yu, C., Chen, M., and Sun, C. (2016). TRIM37 promoted the growth and migration of the pancreatic cancer cells. *Tumour Biol. J. Int. Soc. Oncodevelopmental Biol. Med.* 37, 2629–2634.
- Kallijärvi, J., Avela, K., Lipsanen-Nyman, M., Ulmanen, I., and Lehesjoki, A.-E. (2002). The TRIM37 gene encodes a peroxisomal RING-B-box-coiled-coil protein: classification of mulibrey nanism as a new peroxisomal disorder. *Am. J. Hum. Genet.* 70, 1215–1228.

- Kallijärvi, J., Lahtinen, U., Hämäläinen, R., Lipsanen-Nyman, M., Palvimo, J.J., and Lehesjoki, A.-E. (2005). TRIM37 defective in mulibrey nanism is a novel RING finger ubiquitin E3 ligase. *Exp. Cell Res.* *308*, 146–155.
- Karlberg, N., Karlberg, S., Karikoski, R., Mikkola, S., Lipsanen-Nyman, M., and Jalanko, H. (2009a). High frequency of tumours in Mulibrey nanism. *J. Pathol.* *218*, 163–171.
- Karlberg, S., Lipsanen-Nyman, M., Lassus, H., Kallijärvi, J., Lehesjoki, A.-E., and Butzow, R. (2009b). Gynecological tumors in Mulibrey nanism and role for RING finger protein TRIM37 in the pathogenesis of ovarian fibrothecomas. *Mod. Pathol. Off. J. U. S. Can. Acad. Pathol. Inc* *22*, 570–578.
- Kim, D., Song, J., Ahn, C., Kang, Y., Chun, C.-H., and Jin, E.-J. (2014). Peroxisomal dysfunction is associated with up-regulation of apoptotic cell death via miR-223 induction in knee osteoarthritis patients with type 2 diabetes mellitus. *Bone* *64*, 124–131.
- Koparir, A., Karatas, O.F., Yuceturk, B., Yuksel, B., Bayrak, A.O., Gerdan, O.F., Sagiroglu, M.S., Gezdirici, A., Kiritay, K., Selcuk, E., et al. (2015). Novel POC1A mutation in primordial dwarfism reveals new insights for centriole biogenesis. *Hum. Mol. Genet.* *24*, 5378–5387.
- Lindqvist, A., Källström, H., and Karlsson Rosenthal, C. (2004). Characterisation of Cdc25B localisation and nuclear export during the cell cycle and in response to stress. *J. Cell Sci.* *117*, 4979–4990.
- Liu, C.-F., Samsa, W.E., Zhou, G., and Lefebvre, V. (2017). Transcriptional control of chondrocyte specification and differentiation. *Semin. Cell Dev. Biol.* *62*, 34–49.
- Luo, Y., and Pelletier, L. (2014). Pericentrin: critical for spindle orientation. *Curr. Biol. CB* *24*, R962-964.
- M'Baya-Moutoula, E., Louvet, L., Metzinger-Le Meuth, V., Massy, Z.A., and Metzinger, L. (2015). High inorganic phosphate concentration inhibits osteoclastogenesis by modulating miR-223. *Biochim. Biophys. Acta* *1852*, 2202–2212.
- M'baya-Moutoula, E., Louvet, L., Molinié, R., Guerrero, I.C., Cerutti, C., Fourdinier, O., Nourry, V., Gutierrez, L., Morlière, P., Mesnard, F., et al. (2018). A multi-omics analysis of the regulatory changes induced by miR-223 in a monocyte/macrophage cell line. *Biochim. Biophys. Acta Mol. Basis Dis.* *1864*, 2664–2678.
- Meitinger, F., Anzola, J.V., Kaulich, M., Richardson, A., Stender, J.D., Benner, C., Glass, C.K., Dowdy, S.F., Desai, A., Shiau, A.K., et al. (2016). 53BP1 and USP28 mediate p53 activation and G1 arrest after centrosome loss or extended mitotic duration. *J. Cell Biol.* *214*, 155–166.
- Nigg, E.A., and Holland, A.J. (2018). Once and only once: mechanisms of centriole duplication and their deregulation in disease. *Nat. Rev. Mol. Cell Biol.* *19*, 297–312.
- Pan, F., Liu, X.-G., Guo, Y.-F., Chen, Y., Dong, S.-S., Qiu, C., Zhang, Z.-X., Zhou, Q., Yang, T.-L., Guo, Y., et al. (2010). The regulation-of-autophagy pathway may influence Chinese stature variation: evidence from elder adults. *J. Hum. Genet.* *55*, 441–447.

- Pugsley, H.R. (2017). Assessing Autophagic Flux by Measuring LC3, p62, and LAMP1 Co-localization Using Multispectral Imaging Flow Cytometry. *J. Vis. Exp. JoVE*.
- Samsa, W.E., Zhou, X., and Zhou, G. (2017). Signaling pathways regulating cartilage growth plate formation and activity. *Semin. Cell Dev. Biol.* 62, 3–15.
- Settembre, C., Artega-Solis, E., Ballabio, A., and Karsenty, G. (2009). Self-eating in skeletal development: implications for lysosomal storage disorders. *Autophagy* 5, 228–229.
- Shu, L., Zhang, H., Boyce, B., and Xing, L. (2013). Ubiquitin E3 ligase Wwp1 negatively regulates osteoblast function by inhibiting osteoblast differentiation and migration. *J. Bone Miner. Res. Off. J. Am. Soc. Bone Miner. Res.* 28, 1925–1935.
- Taïbi, F., Metzinger-Le Meuth, V., Massy, Z.A., and Metzinger, L. (2014). miR-223: An inflammatory oncomiR enters the cardiovascular field. *Biochim. Biophys. Acta* 1842, 1001–1009.
- Tang, S.-L., Gao, Y.-L., and Wen-Zhong, H. (2018). Knockdown of TRIM37 suppresses the proliferation, migration and invasion of glioma cells through the inactivation of PI3K/Akt signaling pathway. *Biomed. Pharmacother. Biomedecine Pharmacother.* 99, 59–64.
- Wang, W., Xia, Z.-J., Farré, J.-C., and Subramani, S. (2017). TRIM37, a novel E3 ligase for PEX5-mediated peroxisomal matrix protein import. *J. Cell Biol.* 216, 2843–2858.
- Wang, W., Xia, Z., Farré, J.-C., and Subramani, S. (2018). TRIM37 deficiency induces autophagy through deregulating the MTORC1-TFEB axis. *Autophagy* 14, 1574–1585.
- Yan, J., Yan, F., Li, Z., Sinnott, B., Cappell, K.M., Yu, Y., Mo, J., Duncan, J.A., Chen, X., Cormier-Daire, V., et al. (2014). The 3M complex maintains microtubule and genome integrity. *Mol. Cell* 54, 791–804.
- Zhao, L., Huang, J., Guo, R., Wang, Y., Chen, D., and Xing, L. (2010). Smurf1 Inhibits Mesenchymal Stem Cell Proliferation and Differentiation into Osteoblasts through JunB Degradation. *J. Bone Miner. Res.* 25, 1246–1256.

TRIM37 in CHON-002 Chondrocytes cell line

